Roles of different mineral seeds in heavy metals removal/recovery from simulated and actual acid mine wastewater

Ziyu Wang, Minwang Laipan*, Mengyao Yuan, Xueya Wan, Min Zhang, Junkang Guo

School of Environmental Science and Engineering, Shaanxi University of Science and Technology, Xi'an 710021, China

* Corresponding author

Dr. Minwang Laipan, E-mail: laipanminwang@sust.edu.cn; Tel: +86 2986132765

Abstract

Heavy metal being immobilized in the lattice of a mineral is beneficial for its removal, recovery, and reuse from wastewater. It is essential to reveal how can heavy metals be transferred into minerals controllably. This work developed a potential way for transforming heavy metals (Cu^{2+}, Pb^{2+}, Ni^{2+}, Zn^{2+}, and Cd^{2+}) in wastewater into solids with high efficiency by introducing crystal seeds. The results of this work demonstrated that the addition of hydrotalcite and paratacamite crystal seeds can enhance heavy metal removal both in simulated and actual acid mine wastewater. The removal rate can be increased by 18-47% and 31.8% for each heavy metal and total heavy metals in the presence of crystal seed, respectively. Additionally, the recovery products of heavy metals
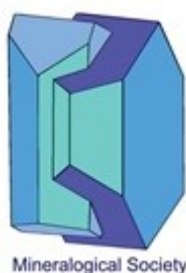
Mineralogical Society

can be changed by crystal seeds. In the systems without crystal seeds, the recovery products are mixtures; but pure phase can be reached when crystal seeds were added. For instance, in Cu^{2+}–Al^{3+}–Cl^- system without crystal seeds, the products were mixtures of paratacamite and layered double hydroxides (LDHs). But the products could be facilely altered by hydrotalcite or paratacamite seeds. Paratacamite seeds induced Cu^{2+} to form paratacamite at pH 5.0, but a mixture of LDHs and paratacamite at pH 7.0. Differently, hydrotalcite seeds induced Cu^{2+} to form LDHs at both pH 5.0 and 7.0. From the perspective of enthalpies of formation, CuAl-LDH and paratacamite are potential products, but the former should be more stable products, and thus it became the dominant products of the reaction systems with crystal seeds. It is believed that the crystal seeds can accelerate the dynamic process of LDHs formation. This work suggests a controllable way for heavy metals removal, recovery, and reuse.

Keywords: heavy metal recycling, crystal seed, precipitation, minerals, fate

1. Introduction

Removal, recycling, and reuse of heavy metal ions from wastewater is an essential component of the goal of environmental protection and sustainability (Tan 2015, Wang et al., 2020a, Wang et al., 2021, Liu et al., 2022). To achieve the goal, various techniques including adsorption (Muhammad et al., 2021, Haris et al., 2022, Zhang et al., 2022b), precipitation (Xu et al., 2023), ion exchange (Guo et al., 2021, Qiu et al., 2022), solvent extraction (de Souza E Silva et al., 2006), membrane separation (Ahmad et al., 2022),

electrochemical means (Wang et al., 2022) and biological approaches (Guo et al., 2020) were developed. In recent years, heavy metal removal based on two-dimensional layered double hydroxides (LDHs) nano-minerals becomes a topic of significant interest due to their extraordinary physiochemical properties (Yu et al., 2017, Laipan et al., 2020). LDHs have been unequivocally proven as promising engineered adsorbents for anionic and cationic heavy metal ions removal (Wan et al., 2016, Siebecker et al., 2018, Laipan et al. 2020, Laipan et al., 2023). Increasing interest therefore, has been paid into the field of preparing novel functionalized LDH with even more exciting adsorptive performance (Wang et al., 2020b, Cai et al., 2023, Laipan et al. 2023). However, few researchers have paid attention to the fact that there are many natural LDHs composed of heavy metal ions in the environment, e.g., Comblainite (NiCo-LDH), Cualstibite (CuAlSb-LDH), Droninoite (NiFe-LDH), Glaucocerinite (ZnAl-LDH), Stichtite (MgCr-LDH), etc. (Mills et al., 2012). Previous studies also demonstrated that a variety of heavy metal ions (e.g., Cu^{2+}, Co^{2+}, Ni^{2+}, Zn^{2+}, Mn^{2+}, and Cd^{2+}) can form LDH under environmental conditions (Goh et al., 2008, Benício et al., 2015, Siebecker et al. 2018). It is further suggested that the immobilization of heavy metals in the mineral lattice can significantly reduce the migration and harmfulness of heavy metals (Towle et al., 1997, Scheckel and Sparks 2001, kumar Allada et al., 2002, Peligro et al., 2016, Siebecker et al. 2018). Therefore, studying the fixation of heavy metals in the structure of LDH during its formation may be more worthy of further exploration than simply using the formed LDH as an adsorbent. Additionally, many studies have shown that LDHs formed by heavy metal ions present

3

varied special physiochemical properties, such as high adsorptive, catalytic, and electrochemical activity, etc. (Laipan et al. 2020) Thus, the conversion of heavy metal ions in waterbody, e.g., wastewater, to LDH may be a promising and effective way to achieve removal, recovery, and reuse of heavy metal.

However, a crucial question is how we can ensure the formation of pure LDH products while maintaining high heavy metal removal efficiency. As the formation of LDH requires trivalent (or higher valence state) and bivalent metal ions, and most heavy metal ions in waterbody are bivalent ions, it may be achievable with the addition of extra trivalent (or higher valence state) metal ions. Indeed, several efforts have been attempted and satisfactory results have been obtained (Zhang et al., 2012, Xu et al., 2013, Sommella et al., 2015, Peligro et al. 2016, Hase et al., 2017). But there are also problems that cannot be ignored that the resulted LDH is impure and it has limited removal efficiency on low concentration of heavy metals. For example, Zhou et al. suggested that heavy metal ions (Ni^{2+}, Zn^{2+}, and Cr^{3+}) can be recovered from real polynary metal ions-bearing electroplating wastewaters as LDH materials via a homogeneous coprecipitation process, but the crystallinity of the LDH is weak and produced impurity phase (Zhou et al., 2010). Zhang et al. attempted to recover Cr(VI) and Zn^{2+} by promoting the formation of Zn-bearing LDH via homogeneous coprecipitation, but also found the weakness of low crystallinity of the product and existence of impurity phase (Zhang et al. 2012). This problem was also confirmed by other researches (Xu et al. 2013, Sommella et al. 2015, Peligro et al. 2016, Hase et al. 2017). Additionally, studies also showed that although 90%

or more heavy metals could be recovered, the residual concentrations may be still at a high level (tens or hundreds mg/L) (Zhang et al. 2012, Peligro et al. 2016). In spite of these drawbacks, these studies still provide a clear and promising direction for the removal/recovery of heavy metals from wastewaters. But how to ensure the purity of the product on the basis of improving the removal efficiency of heavy metals with low concentration is still a big challenge.

Previous researches indicated that the adsorption process can sufficiently enrich concentration of ions around the solid surface, which then can cause a local supersaturated state and induce the formation of surface precipitates (Yan et al., 2017, Siebecker et al. 2018, Deng et al., 2019). Therefore, we proposed that the addition of solid materials in the solution system during coprecipitation of heavy metals may be able to gather the metal ions around solid's surface, resulting in a local supersaturation. In this way, heavy metals with low concentration level may be recoverable by LDH formation method, but how can we ensure that the product is LDH? Crystal seed-induced crystallization may be a potential solution. The crystal seed-assisted crystallization is a kind of "heteroepitaxy." Besides aggregating heavy metals, the hetero-surface of a crystal seed can act as crystal nucleus and provides active sites, so nucleation becomes energetically favorable and therefore will change the crystallization behavior and accelerate the crystallization process (Yazdanpanah et al., 2017). It has been demonstrated that the addition of crystal seeds during crystal synthesis could (i) enhance the crystallization rate, (ii) suppress the formation of undesired phases, and (iii) cause local oversaturation of a low concentration

5

solution via its adsorption or other effects, and thus results in induced crystallization (Li et al., 2015). Consequently, it is possible that heavy metals (even at a low concentration) can be efficiently and rapidly recovered while producing pure crystals by a crystal seed induction method.

Therefore, we took hydrotalcite (one typical type of LDHs) as crystal seeds in this work to verify if heavy metals can be efficiently recovered while producing pure LDH. First, simulated wastewater with various heavy metal ions (Cu^{2+}, Pb^{2+}, Ni^{2+}, Zn^{2+}, and Cd^{2+}) and an actual acid mine drainage were used to test whether the hydrotalcite seeds induction method is applicable to actual wastewaters. Al^{3+} was taken as trivalent metal ion; removal efficiency and recovered product of the heavy metals were compared with homogeneous coprecipitation method (i.e., without hydrotalcite seeds). Second, Cu^{2+} was taken as an example of heavy metal ions to determine the impacts of different crystal seeds to check if crystal seeds can suppress the formation of undesired phases or induce the formation of the target phase. As crystalline hydroxide metal salts (HMSs, $[M_x(OH)_y(X)_z \cdot nH_2O$ (M: metal, X: anion)]) that commonly found in soil environment can also be easily formed by heavy metals (Altmaier et al., 2003, Lin et al., 2005, Georgaka and Spanos 2010), we selected it as another crystal seed. Finally, enthalpies of formation from the elements ($\Delta f\, H°$ at 298.15 K) of different recovered products were employed to discuss the different crystallization behaviors of heavy metal ions. The results of this work demonstrated that LDH seed method can be a well solution for low concentration heavy metals removal/recovery while producing pure LDH product, achieving the goal of

6

removal, recovery, and reuse of heavy metals in wastewater.

2. Materials and methods

2.1 Materials

$Cu(NO_3)_2 \cdot 3H_2O$ (99.0%), $CuCl_2 \cdot 2H_2O$ (99.0%), $Al(NO_3)_3 \cdot 9H_2O$ (99.0%), $AlCl_3 \cdot 6H_2O$ (99.0%), $Mg(NO_3)_2 \cdot 6H_2O$ (99.0%), $Zn(NO_3)_2 \cdot 6H_2O$ (99.0%), $Ni(NO_3)_2 \cdot 6H_2O$ (99.0%), $Cd(NO_3)_2 \cdot 4H_2O$ (99.0%), $Pb(NO_3)_2$ (99.0%), $NaNO_3$ (99.0%), and $NaCl$ (99.0%) were purchased from Aladdin–E. NaOH, HCl, and HNO_3 were purchased from Guangzhou chemical reagent CO., LTD (Guangzhou, China). All chemical reagents were used as received. Crystal seed of hydrotalcite were synthesized by traditional coprecipitation method (Laipan et al., 2015, Laipan et al. 2023, Laipan et al., 2024), and paratacamite (one type of HMSs) were obtained by direct precipitation method (Pollard et al., 1989). Acid mine drainage was collected from Fenghuang Village, Baihe County, Ankang City, Shaanxi Province, China. The concentration of the heavy metals of the acid mine drainage are shown in Table 1.

Table 1 Heavy metal ions and their concentrations of the acid mine drainage

Heavy metal ions	Zn^{2+}	Cr^{6+}	Fe^{3+}	Cu^{2+}
Concentration (mg/L)	53.16	6.94	5059.00	24.35

2.2 Recovery of heavy metals from simulated wastewater by hydrotalcite seed method

1 L solution (pH 3.0) of simulated wastewater with various heavy metal ions (Cu^{2+}, Pb^{2+}, Ni^{2+}, Zn^{2+}, and Cd^{2+}; each concentration of 1 mmol/L) and Al^{3+} (2.5 mmol/L) was

7

prepared by using nitrates. Subsequently, 0.5 g of hydrotalcite seeds were added into the solution while adjusting the reaction pH (using 0.1 mol/L NaOH and HNO$_3$ solution) by an automatic pH controller (Chroma CPH–2, China), and reacted for 12 h under magnetic stirring. To explore the effect of pH, the target reaction pH was maintained at 5~9. After that, the products were centrifuged to obtain the solids and supernatant. The supernatant was used to determine the removal efficiency of various heavy metals by ICP-MS (Agilent 7900), while the solid products were finally freeze dried for further analysis after washing with ultrapure water for three times. Reaction system with pH 7.0 was also used to observe removal kinetic process of each heavy metals. The concentrations of the heavy metal cations in the supernatant were determined by sampling at intervals of 1, 2, 5, 10, 15, 30, 45, 60, 120, and 180 minutes.

Controlled experiments without adding hydrotalcite seeds were also conducted. The experimental procedure kept the same with the above experiments; the only difference is that no crystal seed is added during the reaction.

2.3 Recovery of heavy metals from acid mine drainage by hydrotalcite seed method

200 mL solution of acid mine drainage was used to conduct the experiment. 0.2 g of hydrotalcite seeds were added into the solution while adjusting the reaction pH to 7.0 (using 0.1 mol/L NaOH solution) by an automatic pH controller (Chroma CPH–2, China). The concentrations of heavy metals in the supernatant were determined (using ICP-MS) by sampling at intervals of 5, 10, 30, 60, 90, 120, and 180 minutes. As there is Fe^{3+} in the drainage, no Al^{3+} was added into the drainage during reaction. Controlled experiments

8

without adding hydrotalcite seeds were also conducted.

2.4 Recovery of Cu^{2+} in the presence of different crystal seeds

Cu^{2+}-Cl^--Al^{3+} system was used to test the effects of different crystal seeds (hydrotalcite and a crystalline hydroxide metal salt of paratacamite) on the recovered products. 1 L solution (pH 4.5) with 5 mM $CuCl_2 \cdot 2H_2O$ and 2.5 mM $AlCl_3 \cdot 6H_2O$ was first prepared with the molar ratio of Cl to Cu to Al is 7:2:1. The crystal seeds of paratacamite or hydrotalcite was then added into the Cu^{2+}-Cl^--Al^{3+} system maintaining a crystal seed concentration of 1 g/L. After that, the solution pH was regulated to the target pH of 5.0 and 7.0, and reacted for 12 h under magnetic stirring. Finally, the products were centrifuged and freeze dried for further analysis.

2.5 Characterization methods

XRD patterns of the products were measured on a Bruker D8 ADVANCE X–ray diffractometer using Cu Kα radiation operating at 40 kV and 40 mA. The patterns were recorded over the 2θ range from 3 to 80° with a scan speed of 3°/min using a bracket sample holder. SEM images were obtained by FEI Verios 460 high-resolution field emission scanning electron microscopy. STEM and elemental mapping images were collected by FEI Talos F200S high-resolution transmission electron microscopy.

3. Results and discussion

3.1 Effects of crystal seeds on heavy metals removal

The impact of hydrotalcite crystal seeds on the removal of heavy metals from simulated wastewater and actual acid mine drainage was assessed. Simulated wastewater

with mixed heavy metal ions (Cu^{2+}, Pb^{2+}, Ni^{2+}, Zn^{2+}, and Cd^{2+}) was used to test whether the hydrotalcite crystal seed method is applicable to the wastewater with multiple heavy metals; also, to reveal if the coexistent heavy metal cations would affect the removal of each other. Results indicated an improvement of heavy metal removal efficiency around pH 7-9 by using crystal seed method (Figure 1 g-j; thus, pH $\geqslant$ 7 was selected in the following experiments). At pH 6, the removal of Cu, Cd, and Pb were improved while Ni and Zn were decreased. Under a more acid solution (e.g., pH 5), the removal of heavy metals was significantly lower than that of the seed-free system. The reasons for the above differences under acid solution (pH 5 and 6) should be that an acid condition would result in dissolution of the hydrotalcite. Additionally, hydrotalcite removes heavy metal cations mainly via ligand exchange with the H^+ (on the surface hydroxyl groups of hydrotalcite), surface precipitation, and isomorphic substitution (Liang et al., 2013, He et al., 2018). Under an acid solution, the ligand exchange between heavy metal cations and surface hydroxyl groups (H^+) would be suppressed by the free H^+ ions and thus caused the decrease of removal rate. According to the experimental results, the addition of hydrotalcite crystal seeds can effectively improve the heavy metals removal efficiencies with an increase of 18%-47%, and for all heavy metals, the total heavy metal removal rate can be increased by 31.8% (Figure 1a-e, under pH 7).

An actual acid mine drainage with the coexistence of heavy metal cations (Fe^{3+}, Cu^{2+}, Zn^{2+}) and anion (Cr(VI)) (Table 1) was also employed to test whether the hydrotalcite crystal seed method is applicable to actual wastewater. Without addition of hydrotalcite

10

crystal seeds, Fe^{3+}, Cu^{2+}, and Cr(VI) can be removed completely by pH neutralization, but the removal rate of Zn^{2+} presented an abnormal decrease trend as reaction time increase (Figure 1k). This abnormal decrease trend can also be found in the previous study about removal of Zn^{2+} by Zn^{2+}-Al^{3+} coprecipitation method(Laipan et al. 2024). However, this abnormal decrease trend can be eliminated by the addition of hydrotalcite crystal seeds (Figure 1l). Our previous research findings indicate that the precipitation of Zn^{2+} and the formation of Zn-LDH are not synchronous, leading to the re-release of Zn^{2+} back into the solution (Laipan et al. 2024). Zn^{2+} may initially form precipitates and be adsorbed onto ferric hydroxide, then gradually evolves into Zn-LDH, during which the formation of positively charged Zn-LDH results in some Zn^{2+} being re-released into the solution. This phenomenon did not occur in simulated wastewater; we speculate that this may be due to the coexistence of five divalent metal ions in the simulated wastewater, including ions with a precipitation pH close to that of Zn^{2+}, which easily leads to the coprecipitation of Zn, forming a multi-component LDH of Zn with one or more of Cu/Ni/Cd/Pb. In actual acid mine wastewater, only Cu^{2+} and Zn^{2+} are present as divalent metal ions, with Cu^{2+} being in a lower concentration (24 ppm for Cu and 53 ppm for Zn). The amount of Zn removed by coprecipitation with Cu^{2+} to form Cu/Zn-LDH should be relatively small. Additionally, the large difference in precipitation pH of Cu^{2+} and Zn^{2+} may inhibit the coprecipitation removal of Zn. Fe^{3+}, Cu^{2+}, and Zn^{2+} can be well removed in the presence of hydrotalcite seeds, but for Cr(VI) its removal decreased as time increase. This is because the removal of Cr(VI) by LDH faces competition from water-soluble carbon

11

dioxide. As indicated by Figure 1l, reaction for 50-60 min should be an effective way for realizing high removal efficiency for all the heavy metals.

3.2 Effects of crystal seed on heavy metal recovery product

The solid products generated from simulated wastewater (with mixed heavy metals of Cu^{2+}, Pb^{2+}, Ni^{2+}, Zn^{2+}, and Cd^{2+}) in the treatments with and without hydrotalcite seeds were characterized by XRD. The results showed that there are two crystalline products of LDH and hydrotalcite hydrocerussite $(Pb_3(CO_3)_2(OH)_2)$ (Figure 2). Without hydrotalcite seeds, the dominant product is hydrocerussite with a small amount of impurity phase of LDH. However, when hydrotalcite seeds were added into the reaction system the dominant recovered product became LDH phase at higher pH, with a small amount of impurity phase of hydrocerussite. During the reaction, only by-product of hydrocerussite was observed, and fortunately, the phase of the recovered products can be regulated by adjusting the reaction pH. The above results suggests that the use of crystal seeds can selectively induce the formation of certain kind of products of heavy metals.
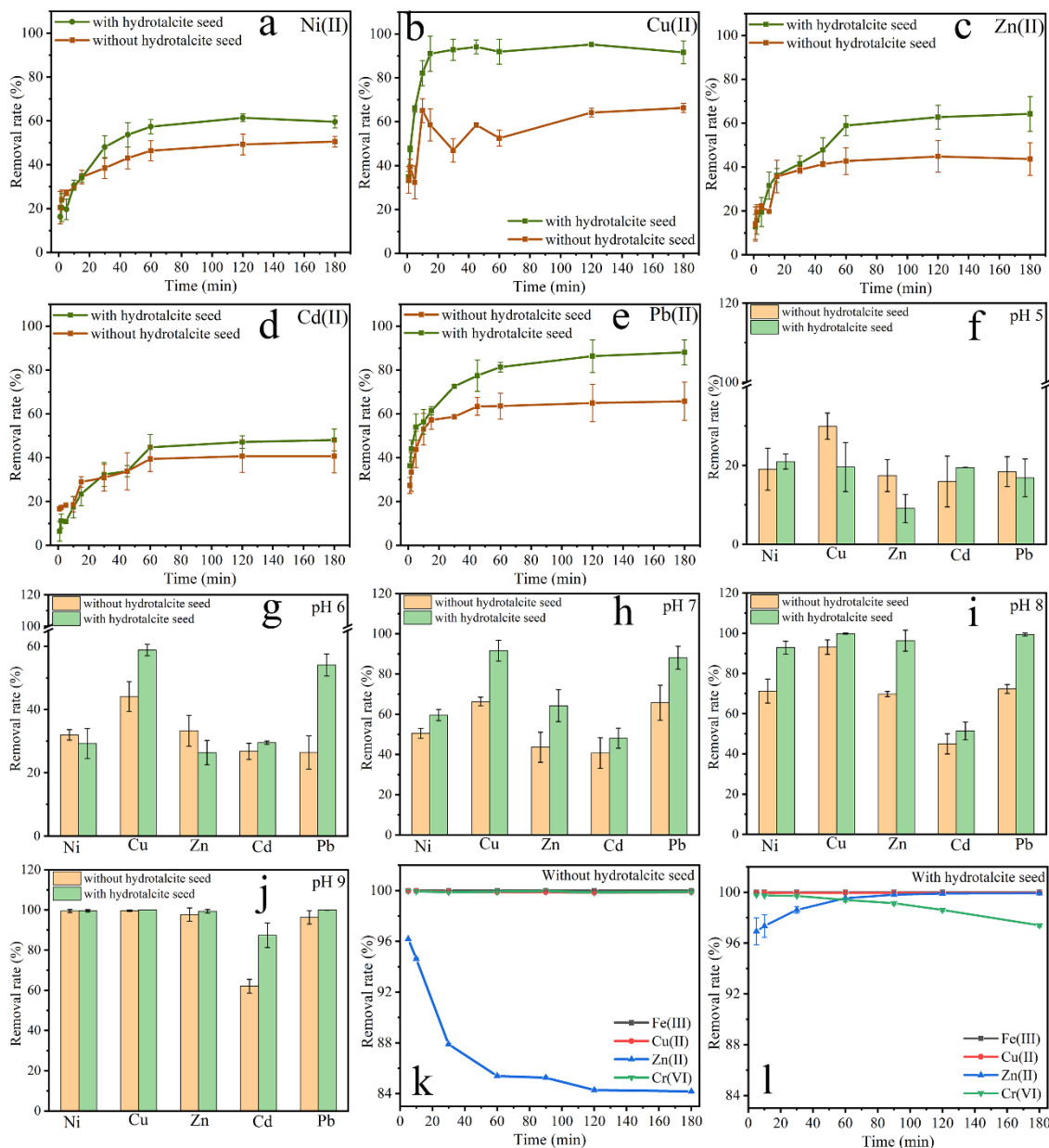
12

Figure 1. Simultaneous removal of multiple heavy metal ions from simulated wastewater and actual acid mine drainage in the systems with and without hydrotalcite seed: (a)~(e) removal kinetics under pH 7 from simulate wastewater; (f)~(j) removal efficiencies under different pH from simulate wastewater; (k) and (l) removal kinetics of multiple heavy metal ions from actual acid mine drainage under pH 7. The concentration of each heavy metal in simulated wastewater is 1 mmol/L; the concentration of hydrotalcite seed in all systems is 1 g/L; the contact time in all systems is 3 h.
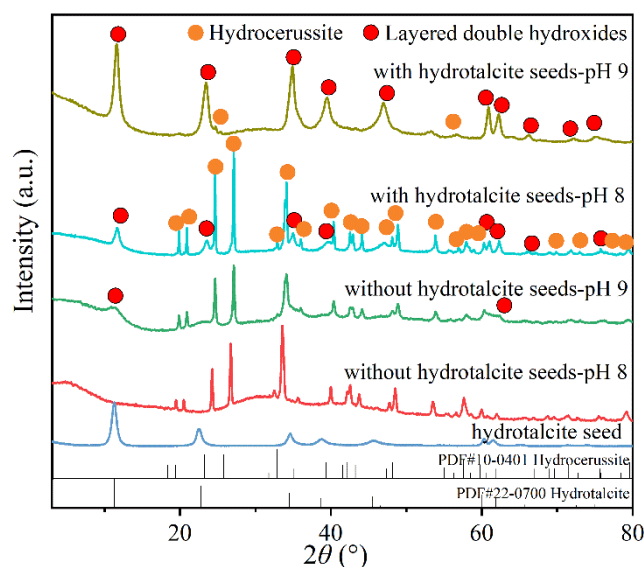
13

Figure 2. XRD patterns of the recovered products from the simulated wastewater with mixed heavy metal ions (Cu^{2+}, Pb^{2+}, Ni^{2+}, Zn^{2+}, and Cd^{2+}) with or without hydrotalcite seeds addition.

To further reveal the effect of crystal seed on product selectivity, a simplified system of Cu^{2+}–Al^{3+}–Cl^- with addition of different crystal seeds is used. Taking into account that copper ions can complete precipitation at low pH generally less than 6.5, the experimental pH values were chosen as 5 and 7. For Cu^{2+}–Al^{3+}–Cl^- reaction system without crystal seeds, the products are mixtures of LDH and paratacamite ($Cu_2(OH)_3Cl$) (Figure 3a). When Cu^{2+} encountered with both Cl^- and Al^{3+}, the dominant crystalline solids are paratacamite with small amount of LDH at low Al^{3+} concentration. But the proportion of LDH increased with increasing Al^{3+} concentration. As LDH and paratacamite are products of Cu^{2+}–Al^{3+}–Cl^- system, LDH (hydrotalcite) and paratacamite were employed as two different kinds of crystal seed. According to Figure 3b, only paratacamite was formed at pH 5.0 when applied paratacamite as crystal seed; but when pH increased to 7.0 the crystalline products reverted to a mixture of LDH and paratacamite, and LDH became the dominant product. Interestingly, when hydrotalcite seeds were added into

14

Cu^{2+}-Cl^--Al^{3+} system, LDH became the only crystalline product at both pH 5.0 and 7.0. Notably, there are two kinds of LDH (i.e., hydrotalcite and CuAl-LDH) in the resultant solid of the hydrotalcite seeding system under pH 7.0, suggested by the two diffraction peaks (at 2θ of c.a. 11°, belonging to (003) of LDH) and their corresponding secondary diffraction peaks (at 2θ of 23-24°, belonging to (006) of LDH). Regarding to the only one diffraction peak belonging to (003) of LDH of the product in hydrotalcite seeding system at pH 5.0, the reason may be the content or concentration of formed CuAl-LDH is low. The above results suggested that crystal seed can change the fate of heavy metal ions by inducing to form specific mineral. That is, the recovered products of heavy metal ions can be controlled by addition of different crystal seeds.
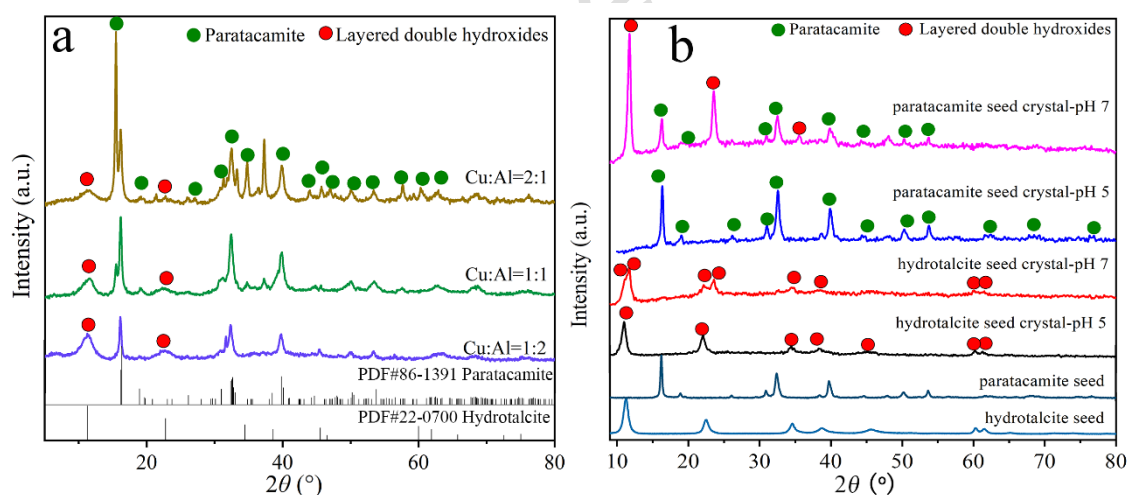

Figure 3 XRD patterns of Cu–bearing minerals generated from different systems: (a) crystalline products from Cu^{2+}–Cl^-–Al^{3+} systems at pH 7.0 with different Cu:Al molar ratio; (b) crystalline products from different crystal seeds (paratacamite and hydrotalcite) induced Cu^{2+}–Cl^-–Al^{3+} systems at pH 5.0 and 7.0 with Cu:Al molar ratio of 2. At pH 5.0, paratacamite induced Cu^{2+} to form paratacamite; at pH 7.0 the products are a mixture of paratacamite and LDH, with LDH as the dominant product. While with hydrotalcite seeds, the products are LDH only both at pH 5.0 and 7.0.

The products were further analyzed by SEM and STEM. Products from paratacamite seeding system at pH 5.0 show not well-developed octahedral nanocrystals-like shape,

15

which is similar with the reported shape of paratacamite particle (Liu et al., 2017), further supporting the formation of paratacamite (Figure 4a, b). Products from paratacamite seeding system at pH 7.0 show both flaky and nano-sized particle morphology, suggesting the coexistence of LDH and paratacamite (Figure 4c, d). When applied hydrotalcite as crystal seed, only flaky morphology belonging to LDH was observed (Figure 4 e-h), indicating the only product of LDH, well in agreement with XRD results.

TEM analysis results also confirm only nano-sized particle shape in the products from paratacamite seeding system at pH 5.0, while coexistence of flaky and particle morphology in the products at pH 7.0 (Figure 5a, b), further demonstrating the crystalline product of paratacamite and mixture of paratacamite and LDH at pH 5.0 and 7.0, respectively. The only flaky morphology in the products from hydrotalcite seeding systems suggests the products are LDH only (Figure 5c, d). Additionally, elemental mapping results provide visual evidence for the formation of different Cu-bearing minerals at different systems. In the paratacamite seeding systems, the distributions of Cu and Cl are highly consistent in the products generated at pH 5.0 (Figure 5e). But in the products resultant from pH 7.0, some of Cu element are highly consistent with Cl in distribution, while more are distributed along with Al (Figure 5f). These results further support the formation of mixture of LDH and paratacamite, and LDH is the dominant product. As for the hydrotalcite seeding systems, all of the Cu, Al, and Cl are highly consistent in distribution in the products (Figure 5g, h), indicating single type of product. Based on the analysis of XRD, SEM, TEM and elemental mapping results, the product

16

should be CuAl-LDH with Cl$^-$ as counterion in the interlayer in the hydrotalcite seeding systems. In summary, addition of crystal seed during heavy metal removal/recovery by precipitation can change the product, and different crystal seeds present different induction effects on product selectivity, which is illustrated in Figure 6.

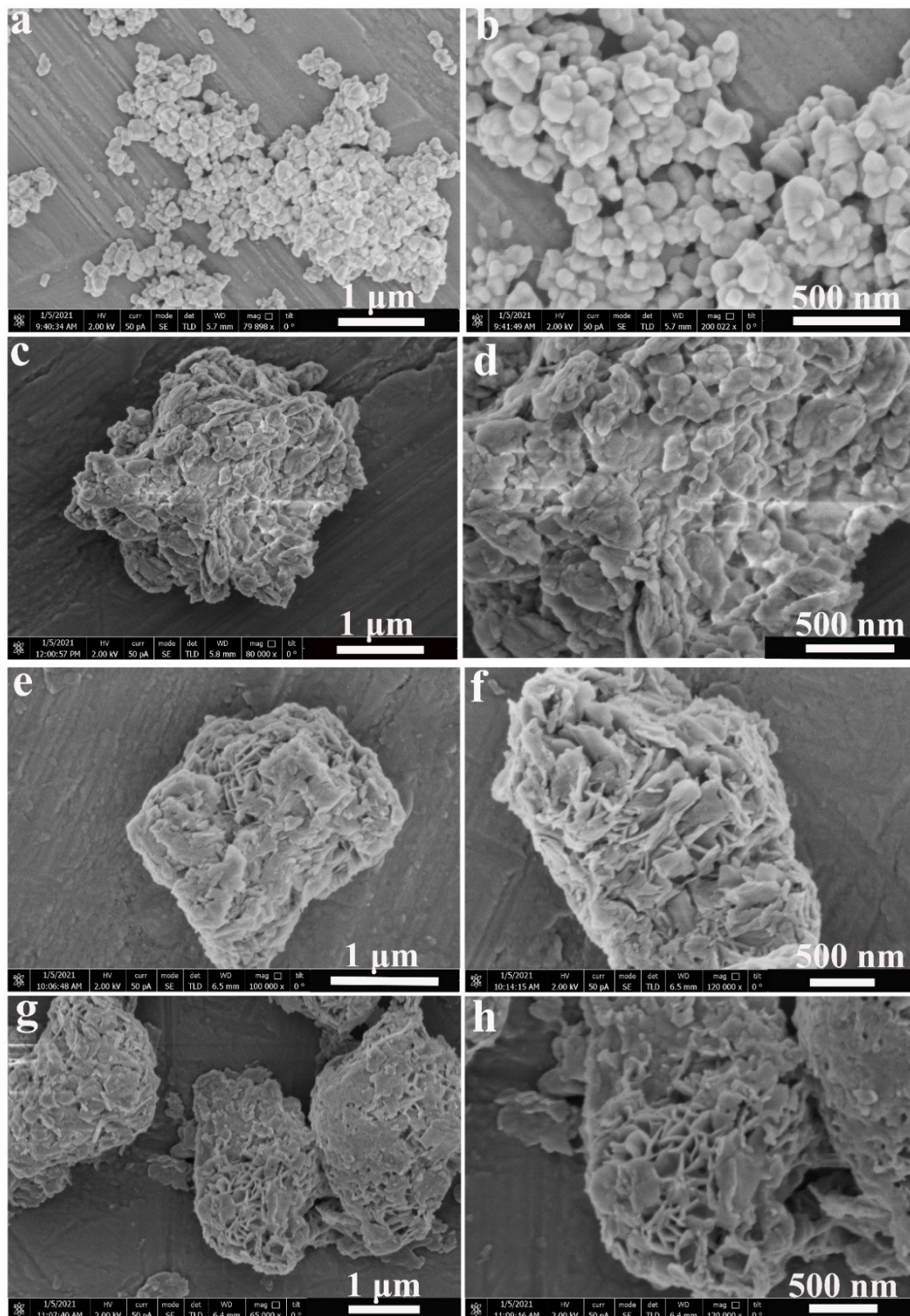Figure 4 SEM images of the Cu-bearing solids produced from the paratacamite and hydrotalcite inducing $Cu^{2+}-Cl^--Al^{3+}$ system at pH 5.0 and 7.0. **a, b**: products from paratacamite system at pH 5.0; **c, d**: products from paratacamite system at pH 7.0; **e, f**: products from hydrotalcite system at pH 5.0; **g, h**: products from hydrotalcite system at pH 7.0.

18
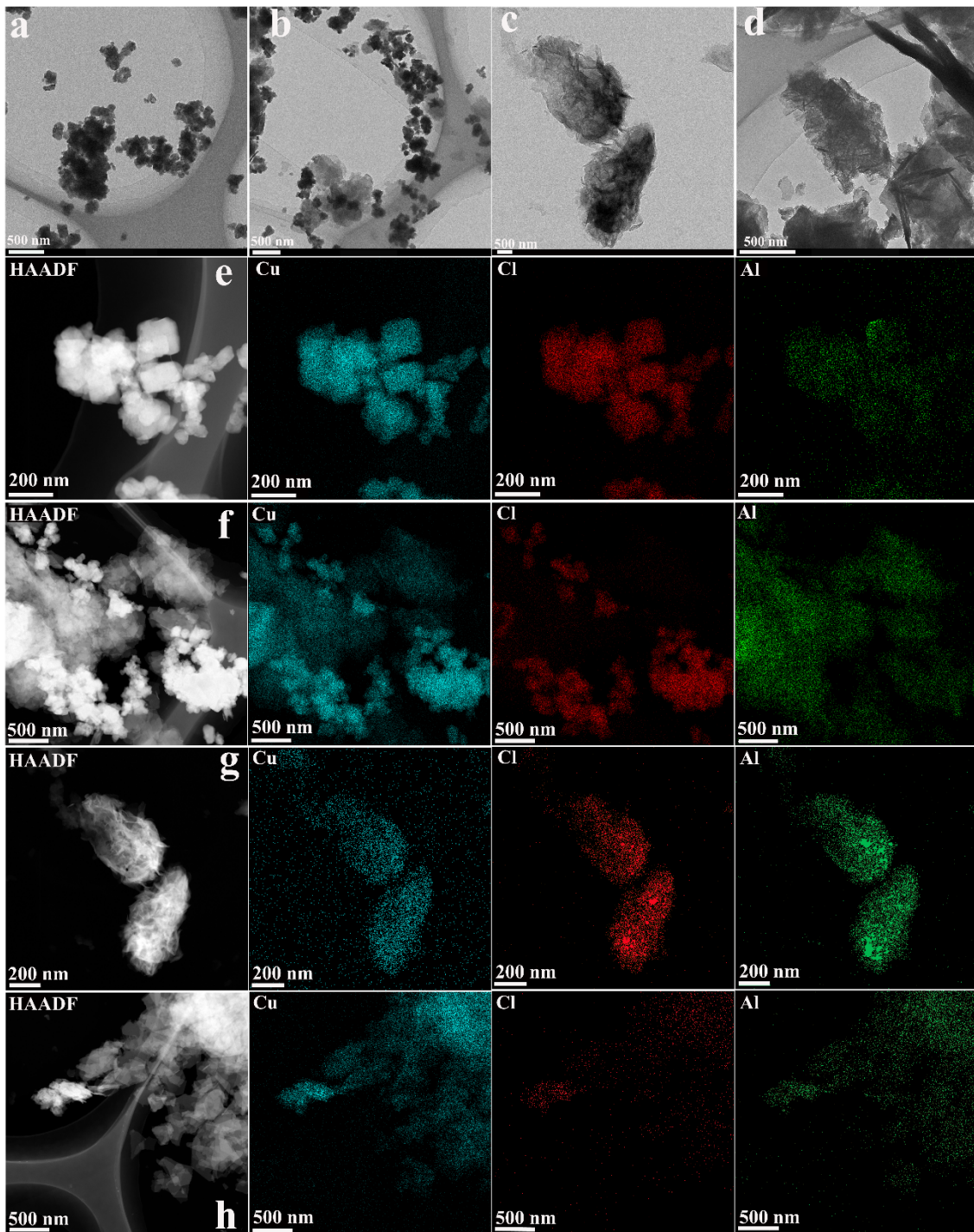
Figure 5. TEM and elemental mapping images of the products of soil mineral inducing Cu^{2+}–Cl^-–Al^{3+} systems. **a, e**: products from paratacamite seed system at pH 5.0; **b, f**: products from paratacamite seed system at pH 7.0; **c, g**: products from hydrotalcite seed system at pH 5.0; **d, h**: products from hydrotalcite seed system at pH 7.0.
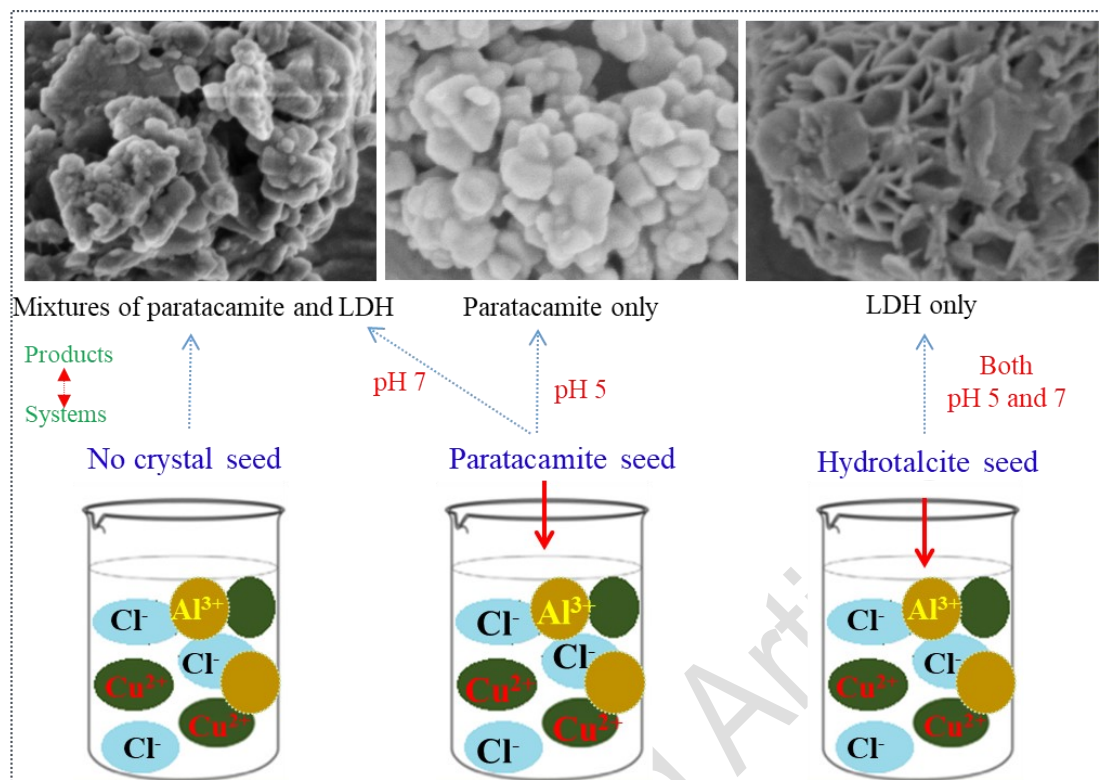
Figure 6. Reaction systems and their corresponding products.

3.3 The relationship between enthalpy of formation and crystallization behavior

Enthalpies of formation from the elements ($\Delta_f H°$ at 298.15 K) of different products were employed to reveal the different crystallization behaviors of Cu^{2+} in the presence of ions and different crystal seeds. In general, thermodynamic properties can be estimated by treating a compound as a mixture of binary compounds in which the metal and anion with similar coordination environments (kumar Allada et al. 2002). For example, for a phase of LDH of $M(II)_{1-x}M(III)_x(OH)_2(A^{n-})_{x/n} \cdot m H_2 O$ (anions, A^{n-}; divalent metal, $M(II)$; trivalent metal, $M(III)$), previous studies indicated that the enthalpies of formation can be estimated as a weighted sum of the components (equation 1) (kumar Allada et al. 2002, Evans and Slade 2006). Therefore, the enthalpies of formation of CuAl-LDH ($Cu_{1-x}Al_x(OH)_2Cl_x \cdot m H_2 O$) and paratacamite ($Cu_2(OH)_3Cl$) can be estimated according to

equations (1) - (3).

$$\Delta_f H^\circ_{M(II)_{1-x}M(III)_x(OH)_2(A^{n-})_{x/n} \cdot mH_2O}$$

$$= \frac{x}{n}\Delta H_{M(II)A_{2/n}} + x\Delta H_{M(III)(OH)_3} + (1-2x)\Delta H_{M(II)(OH)_2} + m\Delta H_{H_2O} \qquad (1)$$

$$\Delta_f H^\circ_{Cu_2(OH)_3Cl} = \frac{1}{2}\Delta H_{CuCl_2} + \frac{3}{2}\Delta H_{Cu(OH)_2} \qquad (2)$$

$$\Delta_f H^\circ_{Cu_{1-x}Al_x(OH)_2Cl_x \cdot mH_2O}$$

$$= \frac{x}{2}\Delta H_{CuCl_2} + x\Delta H_{Al(OH)_3} + \left(1 - \frac{3x}{2}\right)\Delta H_{Cu(OH)_2} + m\Delta H_{H_2O} \qquad (3)$$

For LDH, according to the previous reports, the value of x is generally in the range 0.2~0.33 (Evans and Slade 2006, Fan et al., 2014), and m=1-(3x/2) (Miyata 1980); the value of m should therefore, be in the range 0.51~0.70. Accordingly, a range of enthalpies of formation of CuAl-LDH can be estimated. The enthalpies of formation of different compounds are given in Table 2 (the enthalpies of formation of the binary compounds are from "Lange's handbook of chemistry" (Dean 1999)). According to the calculation, $Cu_2(OH)_3Cl$ possess much lower enthalpies of formation (–778.6 KJ/mol) than that of $Cu(OH)_2$ (–450.4 KJ/mol), indicating paratacamite is more stable and thermodynamic favorable. CuAl-LDH and paratacamite present close values of enthalpies of formation; this should be the reason for the fact that the product of Cu^{2+}–Cl^-–Al^{3+} systems are a mixture of paratacamite and LDH. Increasing the concentrations of Al^{3+} in Cu^{2+}–Al^{3+}–Cl^- systems will generally increase the x value of CuAl-LDH ($Cu_{1-x}Al_x(OH)_2Cl_x \cdot mH_2$O), and thus favors the formation of LDH, well in agreement with XRD results (Figure 3a).

Table 2. Enthalpies of formation (298.15 K) from hydroxide and chlorate components, and elements.

Sample	$\Delta_f H^\circ$ (KJ/mol)	Sample	$\Delta_f H^\circ$ (KJ/mol)
CuCl$_2$	–206.0	H$_2$O	–285.8

Cu(OH)$_2$	–450.4	Cu$_2$(OH)$_3$Cl	–778.6
Al(OH)$_3$	–1285.1	Cu$_{1-x}$Al$_x$(OH)$_2$Cl$_x$ mH$_2$O	–829.9 ~ –793.0

However, as enthalpies of formation of CuAl-LDH (–829.9 ~ –793.0 KJ/mol) is slightly lower than that of paratacamite (–778.6 KJ/mol), the former has higher stability than the latter. Thus, the dominant product should be LDH instead of paratacamite in Cu^{2+}–Cl$^-$–Al^{3+} systems without crystal seeds. But it was suggested by the results that the paratacamite was the dominant product in these systems without crystal seeds. The following two reasons may be responsible for why the theory does not agree with the fact. On the one hand, it is widely believed that the metal hydroxide is formed first and subsequently crystalizes into LDH (Boclair and Braterman 1999, Boclair et al., 1999, Evans and Slade 2006, Yang et al., 2011, Chang et al., 2013, Grégoire et al., 2013, Paikaray et al., 2014). As suggested by the enthalpies of formation of Cu(OH)$_2$ and Cu$_2$(OH)$_3$Cl, the latter is more thermodynamic favorable products. Therefore, paratacamite will form first which prevents the formation of Cu(OH)$_2$, and eventually prevents the formation of CuAl-LDH. On the other hand, the formation of CuAl-LDH may be controlled primarily by dynamics rather than thermodynamics, and paratacamite may be more dynamics preferable products than CuAl-LDH. The addition of crystal seeds can change products may be due to the fact that the hetero-surface of crystal seeds can act as crystal nucleus and provides active sites, so nucleation becomes energetically favorable and therefore will change the crystallization behavior and accelerate the crystallization process (Yazdanpanah et al. 2017).

3.4 Possible reason for the induction effect of crystal seed on heavy metal removal

22

and product

According to the results of this work, the addition of hydrotalcite and paratacamite crystal seeds both can enhance the removal of heavy metals and crystallization of products, and the types of the product is closely related to the types of the added crystal seed. It is believed that the following aspects may be the cause of the improvement of heavy metal removal efficiency by crystal seed method: (1) the crystal seed is also a adsorbent with high surface reactivity that can rapidly accumulate ions on its surface (Zhang et al., 2022a, Laipan et al. 2023, Li et al., 2023); thus, local supersaturation may be easily reached, leading to interfacial precipitation or co-precipitation. As indicated in the introduction, adsorption, the commonly occurring process in the nature, can sufficiently enrich concentration of ions around the solid surface, causing a local supersaturated state and formation of surface precipitates (Yan et al. 2017, Siebecker et al. 2018, Deng et al. 2019). (2) The addition of hydrotalcite seeds can promote the heterogeneous nucleation pathway of a crystal, increasing the crystallization efficiency and growth process of a crystal (Sear 2006, Yazdanpanah et al. 2017). Additionally, the seeds can also cause local oversaturation of a low concentration solution via its adsorption or other effects, and thus results in induced crystallization (Li et al. 2015, Deng et al. 2019). (3) Previous studies have demonstrated that under a solid-water interface the solid could well induced the crystallization of ions even under a low saturated or unsaturated solution environment (Qian and Botsaris 1998, Liu et al., 2021, Yang et al., 2023). This may be due to the adding of crystal seeds can provide extra surface energy (Yazdanpanah et al. 2017). The

23

extra surface energy may also be the reason for the different crystallization behaviors of systems with and without paratacamite and hydrotalcite seeds.

4. Conclusions

The results of this work demonstrated that the addition of crystal seeds can enhance heavy metal removal both in simulated and actual acid mine wastewater and possesses high potential in changing the fate of heavy metal ion. In mixed heavy metal wastewater, the removal rate of each heavy metal can be increased by 18-47% in the presence of crystal seed. And for all heavy metals, the total heavy metal removal rate can be increased by 31.8%. Additionally, the addition of crystal seeds can also control the recovery products of heavy metals. In the reaction systems without crystal seeds, the recovery products are mixtures of two different crystalline phases, but one of the crystalline phases can be eliminated by the addition of crystal seeds, leading to the formation of pure phase of product. For instance, in Cu^{2+}–Al^{3+}–Cl^- system, the crystalline products were mixtures of paratacamite and LDH without crystal seeds addition. But the products could be facilely altered by the hydrotalcite or paratacamite seeds. Paratacamite crystal seeds induced Cu^{2+} to form paratacamite at pH 5.0, but a mixture of LDH and paratacamite at pH 7.0. Differently, hydrotalcite crystal seeds induced Cu^{2+} to form LDH at both pH 5.0 and 7.0. From the perspective of enthalpies of formation, the formation of CuAl-LDH may be controlled primarily by dynamics rather than thermodynamics, and paratacamite may be more dynamics preferable products than CuAl-LDH. The addition of crystal seeds can change the reaction pathway of heavy metals, and it is believed that the crystal seeds

24

can accelerate the dynamic process of LDH formation. This work suggests a potential controllable way for heavy metals removal, recovery, and reuse.

Conflicts of interest

There are no conflicts to declare.

Acknowledgment

Author Contributions

Ziyu Wang performed the experiment and wrote the manuscript. Minwang Laipan conceived and designed the experiments, analyzed the data, and edited the manuscript. Min Zhang, Mengyao Yuan, and Xueya Wan performed the characterization section. Junkang Guo edited the manuscript.

References

Ahmad, N. N. R., W. L. Ang, Y. H. Teow, A. W. Mohammad and N. Hilal (2022). "Nanofiltration membrane processes for water recycling, reuse and product recovery within various industries: A review." Journal of Water Process Engineering **45**: 102478.

Altmaier, M., V. Metz, V. Neck, R. Müller and T. Fanghänel (2003). "Solid-liquid equilibria of Mg (OH) 2 (cr) and Mg2 (OH) 3Cl· 4H2O (cr) in the system Mg-Na-H-OH-Cl-H2O at 25 C." Geochimica et Cosmochimica Acta **67**(19): 3595-3601.

Benício, L. P. F., R. A. Silva, J. A. Lopes, D. Eulálio, R. M. M. d. Santos, L. A. d. Aquino, L. Vergütz, R. F. Novais, L. M. d. Costa and F. G. Pinto (2015). "Layered double hydroxides: nanomaterials for applications in agriculture." Revista Brasileira de Ciência do Solo **39**(1): 1-13.

Boclair, J. W. and P. S. Braterman (1999). "Layered double hydroxide stability. 1. Relative stabilities of layered double hydroxides and their simple counterparts." Chemistry of Materials **11**(2): 298-302.

Boclair, J. W., P. S. Braterman, J. Jiang, S. Lou and F. Yarberry (1999). "Layered double hydroxide stability. 2. Formation of Cr (III)-containing layered double hydroxides directly from solution." Chemistry of Materials **11**(2): 303-307.

Cai, H., K. Ma, Y. Zhang, X. Li, W. Wang and S. Tong (2023). "Carbonizing hollow metal–organic framework/layered double hydroxide (MOF/LDH) nanocomposite with excellent adsorption capacity for removal of Pb (II) and organic dyes from wastewater." Carbon Research **2**(1): 23.

Chang, Z., C. Wu, S. Song, Y. Kuang, X. Lei, L. Wang and X. Sun (2013). "Synthesis mechanism study of layered double hydroxides based on nanoseparation." Inorganic chemistry **52**(15): 8694-8698.

de Souza E Silva, P. T., N. T. de Mello, M. M. Menezes Duarte, M. C. B. S. M. Montenegro, A. N. Araujo, B. de Barros Neto and V. L. da Silva (2006). "Extraction and recovery of chromium from electroplating sludge." Journal of hazardous materials **128**(1): 39-43.

Dean, J. A. (1999). Lange's handbook of chemistry, New york; London: McGraw-Hill, Inc.

Deng, N., A. G. Stack, J. Weber, B. Cao, J. J. De Yoreo and Y. Hu (2019). "Organic-mineral interfacial chemistry drives heterogeneous nucleation of Sr-rich (Ba-x, Sr1-x)SO4 from undersaturated solution." Proceedings of the National Academy of Sciences of the United States of America **116**(27): 13221-13226.

Evans, D. G. and R. C. Slade (2006). Structural aspects of layered double hydroxides. Layered double hydroxides, Springer**:** 1-87.

Fan, G., F. Li, D. G. Evans and X. Duan (2014). "Catalytic applications of layered double hydroxides: recent advances and perspectives." Chemical Society Reviews **43**(20): 7040-7066.

Georgaka, A. and N. Spanos (2010). "Study of the Cu (II) removal from aqueous solutions by adsorption on titania." Global Nest J **12**(3): 239.

Goh, K. H., T. T. Lim and Z. Dong (2008). "Application of layered double hydroxides for removal of oxyanions: A review." Water Research **42**(6): 1343-1368.

Grégoire, B., C. Ruby and C. Carteret (2013). "Hydrolysis of mixed Ni 2+–Fe 3+ and Mg 2+–Fe 3+ solutions and mechanism of formation of layered double hydroxides." Dalton Transactions **42**(44): 15687-15698.

Guo, J., L. Wang, Y. Tu, H. Muhammad, X. Fan, G. Cao and M. Laipan (2021). "Polypyrrole modified bentonite nanocomposite and its application in high-efficiency removal of Cr (VI)." Journal of Environmental Chemical Engineering **9**(6): 106631.

Guo, J., J. Zhao, X. Ren, H. Jia, H. Muhammad, X. Lv, T. Wei and L. Hua (2020). "Effects of Burkholderia sp. D54 on growth and cadmium uptake of tomato, ryegrass and soybean plants." International journal of environmental science and technology **17**: 1149-1158.

Haris, M., Y. Hamid, L. Wang, M. Wang, N. Yashir, F. Su, A. Saleem, J. Guo and Y. Li (2022). "Cd diminution through microbial mediated degraded lignocellulose maize straw: Batch adsorption and bioavailability trails." Journal of Environmental Management **302**: 114042.

Hase, H., T. Nishiuchi, T. Sato, T. Otake, T. Yaita, T. Kobayashi and T. Yoneda (2017). "A novel method for remediation of nickel containing wastewater at neutral conditions." Journal of Hazardous Materials **329**: 49-56.

He, X., X. Qiu, C. Hu and Y. Liu (2018). "Treatment of heavy metal ions in wastewater using layered double hydroxides: A review." Journal of Dispersion Science and Technology **39**(6): 792-801.

kumar Allada, R., A. Navrotsky, H. T. Berbeco and W. H. Casey (2002). "Thermochemistry and aqueous solubilities of hydrotalcite-like solids." Science **296**(5568): 721-723.

Laipan, M., Q. Chen, Z. Wang, M. Zhang, M. Yuan, R. Zhu and L. Sun (2023). "Interlayer Anions of Layered Double Hydroxides as Mobile Active Sites To Improve the Adsorptive Performance toward Cd2+." Inorganic

Chemistry **62**(34): 13857-13866.

Laipan, M., J. Yu, R. Zhu, J. Zhu, A. T. Smith, H. He, D. O'Hare and L. Sun (2020). "Functionalized layered double hydroxides for innovative applications." Materials Horizons **7**(3): 715-745.

Laipan, M., M. Zhang, Z. Wang, R. Zhu and L. Sun (2024). "Highly efficient recovery of Zn2+/Cu2+ from water by using hydrotalcite as crystal seeds." The Science of the total environment **914**: 169954-169954.

Laipan, M., R. Zhu, Q. Chen, J. Zhu, Y. Xi, G. A. Ayoko and H. He (2015). "From spent Mg/Al layered double hydroxide to porous carbon materials." Journal of Hazardous Materials **300**: 572-580.

Li, Y., H. Sun, Y. Wang, B. Xu and Z. Yan (2015). "Green Routes for Synthesis of Zeolites." Progress in Chemistry **27**(5): 503-510.

Li, Z., Y. Jing, X. Zhang, R. Zhu, J. Yu, J. Chen and X. Qiu (2023). "Recyclable and reusable layered double hydroxide beads for soil remediation: Conveying belt recovery model, mechanism, bioavailability and microbial communities." Journal of Environmental Chemical Engineering **11**(5): 110693.

Liang, X., Y. Zang, Y. Xu, X. Tan, W. Hou, L. Wang and Y. Sun (2013). "Sorption of metal cations on layered double hydroxides." Colloids and Surfaces A: Physicochemical and Engineering Aspects **433**: 122-131.

Lin, X., R. C. Burns and G. A. Lawrance (2005). "Heavy Metals in Wastewater: The Effect of Electrolyte Composition on the Precipitation of Cadmium(II) Using Lime and Magnesia." Water Air & Soil Pollution **165**(1-4): 131-152.

Liu, J., S. Inoué, R. Zhu, H. He and M. F. Hochella Jr (2021). "Facet-specific oxidation of Mn (II) and heterogeneous growth of manganese (oxyhydr) oxides on hematite nanoparticles." Geochimica et Cosmochimica Acta **307**: 151-167.

Liu, X., L. Xu, Y. Huang, H. Cheng and H. J. Seo (2017). "Paratacamite phase stability and improved optical properties of Cu2 (OH) 3Cl crystal via Ni-doping." Materials & Design **121**: 194-201.

Liu, Z., Z. Xu, L. Xu, F. Buyong, T. C. Chay, Z. Li, Y. Cai, B. Hu, Y. Zhu and X. Wang (2022). "Modified biochar: synthesis and mechanism for removal of environmental heavy metals." Carbon Research **1**(1): 8.

Mills, S. J., A. G. Christy, J. M. R. Genin, T. Kameda and F. Colombo (2012). "Nomenclature of the hydrotalcite supergroup: natural layered double hydroxides." Mineralogical Magazine **76**(5): 1289-1336.

Miyata, S. (1980). "Physico-chemical properties of synthetic hydrotalcites in relation to composition." Clays and Clay minerals **28**: 50-56.

Muhammad, H., T. Wei, G. Cao, S. Yu, X. Ren, H. Jia, A. Saleem, L. Hua, J. Guo and Y. Li (2021). "Study of soil microorganisms modified wheat straw and biochar for reducing cadmium leaching potential and bioavailability." Chemosphere **273**: 129644.

Paikaray, S., M. A. Gomez, M. J. Hendry and J. Essilfie-Dughan (2014). "Formation mechanism of layered double hydroxides in Mg2+-, Al3+-, and Fe3+-rich aqueous media: Implications for neutralization in acid leach ore milling." Applied Clay Science **101**: 579-590.

Peligro, F. R., I. Pavlovic, R. Rojas and C. Barriga (2016). "Removal of heavy metals from simulated wastewater by in situ formation of layered double hydroxides." Chemical Engineering Journal **306**: 1035-1040.

Pollard, A., R. Thomas and P. Williams (1989). "Synthesis and stabilities of the basic copper (II) chlorides atacamite, paratacamite and botallackite." Mineralogical magazine **53**(373): 557-563.

Qian, R.-Y. and G. D. Botsaris (1998). "Nuclei breeding from a chiral crystal seed of NaClO3." Chemical engineering science **53**(9): 1745-1756.

Qiu, M., L. Liu, Q. Ling, Y. Cai, S. Yu, S. Wang, D. Fu, B. Hu and X. Wang (2022). "Biochar for the removal of contaminants from soil and water: a review." Biochar **4**(1): 19.

27

Scheckel, K. G. and D. L. Sparks (2001). "Dissolution kinetics of nickel surface precipitates on clay mineral and oxide surfaces." Soil Science Society of America Journal **65**(3): 685-694.

Sear, R. P. (2006). "Heterogeneous and homogeneous nucleation compared: Rapid nucleation on microscopic impurities." The Journal of Physical Chemistry B **110**(10): 4985-4989.

Siebecker, M. G., W. Li and D. L. Sparks (2018). The Important Role of Layered Double Hydroxides in Soil Chemical Processes and Remediation: What We Have Learned Over the Past 20 Years. Advances in Agronomy, vol 147. **147**: 1-59.

Sommella, A., A. G. Caporale, M. A. Denecke, S. Mangold, M. Pigna, A. Santoro, R. Terzano and A. Violante (2015). "Nature and reactivity of layered double hydroxides formed by coprecipitating Mg, Al and As(V): Effect of arsenic concentration, pH, and aging." Journal of Hazardous Materials **300**: 504-512.

Tan, Q. L., Jinhui (2015). "Recycling metals from wastes: a novel application of mechanochemistry." J Environmental science technology **49**(10): 5849-5861.

Towle, S. N., J. R. Bargar, G. E. Brown and G. A. Parks (1997). "Surface precipitation of Co(II)(aq) on Al2O3." Journal of Colloid and Interface Science **187**(1): 62-82.

Wan, J., S. D. Lacey, J. Dai, W. Bao, M. S. Fuhrer and L. Hu (2016). "Tuning two-dimensional nanomaterials by intercalation: materials, properties and applications." Chemical Society Reviews **45**(24): 6742-6765.

Wang, B., F. Liu, F. Zhang, M. Tan, H. Jiang, Y. Liu and Y. Zhang (2022). "Efficient separation and recovery of cobalt(II) and lithium(I) from spent lithium ion batteries (LIBs) by polymer inclusion membrane electrodialysis (PIMED)." Chemical Engineering Journal **430**: 132924.

Wang, J., Y. Chen, T. Sun, A. Saleem and C. Wang (2021). "Enhanced removal of Cr (III)-EDTA chelates from high-salinity water by ternary complex formation on DETA functionalized magnetic carbon-based adsorbents." Ecotoxicology and Environmental Safety **209**: 111858.

Wang, J., D. Zhang, S. Liu and C. Wang (2020a). "Enhanced removal of chromium(III) for aqueous solution by EDTA modified attapulgite: Adsorption performance and mechanism." Science of the Total Environment **720**: 137391.

Wang, Y., J. Kang, S. Jiang, H. Li, Z. Ren, Q. Xu, Q. Jiang, W. Liu, R. Li and Y. Zhang (2020b). "A composite of Ni–Fe–Zn layered double hydroxides/biochar for atrazine removal from aqueous solution." Biochar **2**: 455-464.

Xu, M., J. Ma, X.-H. Zhang, G. Yang, L.-L. Long, C. Chen, C. Song, J. Wu, P. Gao and D.-X. Guan (2023). "Biochar-bacteria partnership based on microbially induced calcite precipitation improves Cd immobilization and soil function." Biochar **5**(1): 20.

Xu, Y., J. Zhang, J. Zhou, C. Chen, Q. Liu, G. Qian and Z. P. Xu (2013). "CN and heavy metal removal through formation of layered double hydroxides from mixed CN-containing electroplating wastewaters and pickle acid liquor." Chemical Engineering Journal **215**: 411-417.

Yan, W., X. Yu, T. Yan, D. Wu, E. Ning, Y. Qi, Y.-F. Han and Q. Li (2017). "A triptycene-based porous hydrogen-bonded organic framework for guest incorporation with tailored fitting." Chemical Communications **53**(26): 3677-3680.

Yang, Y., J. Liu, R. Zhu, Q. Chen, H. Wei, M. Chen, H. Xian and H. He (2023). "Surface-induced oxidation of Mn (II) and crystallization of manganese (hydr) oxides on clay minerals." Geochimica et Cosmochimica Acta **363**: 129-146.

Yang, Y., X. Zhao, Y. Zhu and F. Zhang (2011). "Transformation mechanism of magnesium and aluminum precursor solution into crystallites of layered double hydroxide." Chemistry of Materials **24**(1): 81-87.

Yazdanpanah, N., C. J. Testa, S. R. Perala, K. D. Jensen, R. D. Braatz, A. S. Myerson and B. L. Trout (2017).

"Continuous heterogeneous crystallization on excipient surfaces." Crystal growth & design **17**(6): 3321-3330.

Yu, J., Q. Wang, D. O'Hare and L. Sun (2017). "Preparation of two dimensional layered double hydroxide nanosheets and their applications." Chemical Society Reviews **46**: 5950-5974.

Zhang, J., Y. Li, J. Zhou, D. Chen and G. Qian (2012). "Chromium (VI) and zinc (II) waste water co-treatment by forming layered double hydroxides: Mechanism discussion via two different processes and application in real plating water." Journal of Hazardous Materials **205**: 111-117.

Zhang, S., J. Chen, J. Yu, Q. Yu and X. Qiu (2022a). "Remediation of Cd-contaminated soil through different layered double hydroxides: The weakness of delamination and mechanism." Journal of Environmental Chemical Engineering **10**(3): 107815.

Zhang, Y., M. Haris, L. Zhang, C. Zhang, T. Wei, X. Li, Y. Niu, Y. Li, J. Guo and X. Li (2022b). "Amino-modified chitosan/gold tailings composite for selective and highly efficient removal of lead and cadmium from wastewater." Chemosphere **308**: 136086.

Zhou, J. Z., Y. Y. Wu, C. Liu, A. Orpe, Q. Liu, Z. P. Xu, G. R. Qian and S. Z. Qiao (2010). "Effective self-purification of polynary metal electroplating wastewaters through formation of layered double hydroxides." Environmental science & technology **44**(23): 8884-8890.